Effect of Carbide Morphology on Grain Refinement in Burnishing

Yoshinori Amano[1], Takahisa Suzuki[1] and Kaori Kawano[1]

[1]*Research and Development, Nippon Steel Corporation, Chiba 293-8511, Japan*

The development of ultrafine microstructures in spherical cementite-ferrite (SA) steel and pearlite (P) steel of AISI 52100 under severe plastic deformation by burnishing process was investigated by means of sequential analysis of sliding strain and SEM/TEM observations. In the SA steel, equiaxed ultrafine ferrite grains were formed at the burnished surface. These ultrafine grains were estimated to be formed by continuous dynamic recrystallization because they consisted of high angle grain boundaries. On the other hand, the P steel maintained initial lamellar structure without equiaxed ultrafine ferrite grains even after 10-pass burnishing. This suggested that lamellar ferrite separated by lamellar cementite with a small misorientation inhibited dynamic continuous recrystallization by restricting active slip systems in P steel.

Keywords: *severe plastic deformation, burnishing, grain refinement, ultrafine microstructure, carbide morphology*

1. Introduction

Severe plastic deformation technique is one of the grain refinement methods for metallic materials. It is known as the process to produce ultrafine microstructures with the grain size of less than 1μm in carbon steel, and it exhibits superior high strength [1)] and toughness [2)]. The mechanism of grain refinement by severe plastic deformation is considered as continuous dynamic recrystallization process [3)]. In this process, dislocation introduction and dislocation recovery proceed simultaneously, and the grain boundaries progress from dislocation cell boundary to random grain boundary.

It is well known that the grain size obtained by continuous dynamic recrystallization has a correlation with the Zener-Hollomon (Z) parameter: $Z = \dot{\varepsilon} \exp(Q/RT)$ [4)], where $\dot{\varepsilon}$ is the strain rate, Q is the apparent activation energy for deformation, T is the deformation temperature and R is the gas constant. Smaller grain size is obtained by deformation under higher Z condition [5)].

In addition, it is reported that initial steel microstructures such as bcc ferrite, pearlite and martensite also affect to the grain size obtained by continuous dynamic recrystallization in carbon steel [6-8)]. This indicates the morphology of ferrite grains and cementite particles have some effect on continuous dynamic recrystallization process, but the mechanism is unclear.

Therefore, in order to focus on the effect of carbide morphology on continuous dynamic recrystallization process, two types of initial microstructure were prepared in this study using a commercial high-carbon steel AISI 52100 (JIS SUJ2). One is SA steel with ferrite and discrete spheroidized cementite. The other is P steel with a fine lamellar structure of ferrite and cementite, so called pearlite.

The burnishing used in this study is a chipless machining process that modifies the surface texture by severe plastic deformation of the burnished material. Using the burnishing method, the microstructural development of SA and P steel under severe plastic deformation was investigated, controlling the amount of the strain by varying the repeated cycles numbers of multi-pass burnishing process.

2. Experimental

2.1 Sample preparation and heat treatment

The chemical composition of test steel is listed in Table1.

Table 1 Chemical composition of AISI 52100 (mass%).

Steel	C	Si	Mn	Cr	Mo	Fe
AISI 52100	1.00	0.20	0.40	1.50	0.03	bal.

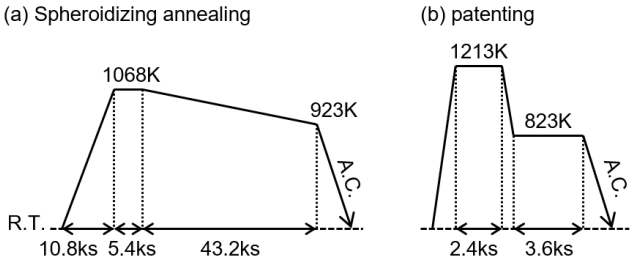

Figure 1 Heat treatments for different microstructure.

(a) Spheroidizing annealing to obtain a spherical cementite-ferrite steel (SA steel).

(b) Patenting to obtain pearlite steel (P steel).

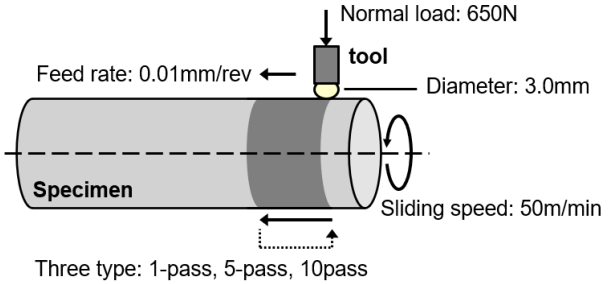

Figure 2 Schematic of burnishing method.

Test steel bars of 30 mm in diameter were normalized at 1173 K for 3.6 ks and air cooled to room temperature. Subsequently, test steel was applied the spheroidizing annealing shown Fig. 1 (a). This was SA steel. Further, P steel was austenitized at 1213K for 2.4 ks and fully transformed to pearlite by isothermal holding at 823K for 3.6ks shown Fig. 1 (b).

2.2 Burnishing process

SA steel and P steel were machined into φ15 × 200 mm bar specimen. Before burnishing, the surface of bar specimens has been finished by turning with cubic boron nitride (CBN) cutting tool at cutting speed: 50 m/min, feed rate: 0.2 mm/rev, depth of cut: 0.1 mm and lubrication with water-soluble cutting oil.

Fig. 2 show the schematic illustration of burnishing

method. A spherical diamond tip with a diameter of 3.0 mm was used. Burnishing was performed with normal load of 650N, sliding speed of 50m/min, feed rate of 0.01mm/rev, and lubrication with water-soluble cutting oil.

Specimens processed with 1-pass, 5-pass and 10-pass burnishing were prepared for each SA steel and P steel. 1-pass of burnishing was defined as burnishing 10mm in the axial direction, and in the multi-pass burnishing, the same 10mm area was processed 5 or 10 times.

2.3 Microstructural observation

The microstructures of the specimens were examined by optical microscopy (OM), scanning electron microscopy (SEM), and transmission electron microscopy (TEM). Observation specimens were cut from the burnished surface of round sections of bars. Specimens for OM were prepared by polishing and etching with a 5% nital solution (5% nitric acid and ethanol). Specimens for SEM were prepared by polishing with colloidal silica (oxide polishing suspension). Specimens for TEM were prepared by focus ion beam (FIB).

3. Result and discussion

Fig. 3 shows the SEM images of microstructures of SA and P steel as heat treated. Although both steels had the same amount of cementite precipitation, the shape and distribution of cementite were different. In the SA steel, spherical cementite having an equivalent circle diameter of about 0.44 μm was dispersed in the matrix ferrite grains. The hardness of the SA steel was about 180 HV. On the other hand, P steel had a fine lamellar structure of ferrite and cementite, and the lamellar spacing was about 0.18 μm. The hardness of the P steel was about 400 HV.

Fig. 4 shows the OM images of microstructures of SA and P steels after 1-pass burnishing at the surface of the round section. In both steels, ferrite and pearlite grains were refined at the surface layer.

In addition, microstructures of both steels were plastically deformed, and plastic flows were in the sliding direction along the dotted line in Figure 4. The depth of plastic flow was about 400μm for SA steel and about 300μm for P steel.

The amount of plastic strain at the surface by burnishing can be estimated from the plastic flows [9]. The amount of the true strain of SA steel at the burnished surface was estimated to be 3.9 for 1-pass, 6.5 for 5-pass, and 10.7 for 10-pass. The amount of true strain increased with the number of burnishing-pass.

In contrast, the amount of the true strain of P steel at the burnished surface was estimated to be 4.3 for 1-pass, 5.2 for 5-pass, and 5.4 for 10-pass. The amount of true strain did not change significantly with the number of burnishing-pass.

Fig. 5 shows TEM images of the microstructures of SA and P steels after 1-pass burnishing and 10-pass burnishing at the surface of round section. SA steel after 1-pass burnishing was composed of equiaxed ultrafine ferrite grains of 230nm in equivalent circle diameter. Fig. 6 (a)-(d) shows diffraction analysis of adjacent ferrite grains in SA steel after 1-pass burnishing. It was revealed that the crystal orientations of these grains were different, and the grain boundaries of these ultrafine grains were high angle boundaries. Therefore, these ultrafine grains were estimated to be formed by continuous

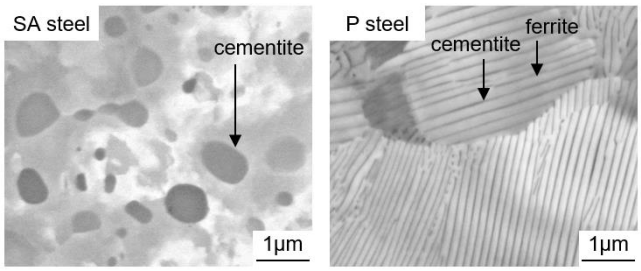

Figure 3 SEM images of SA and P steels as heat treated.

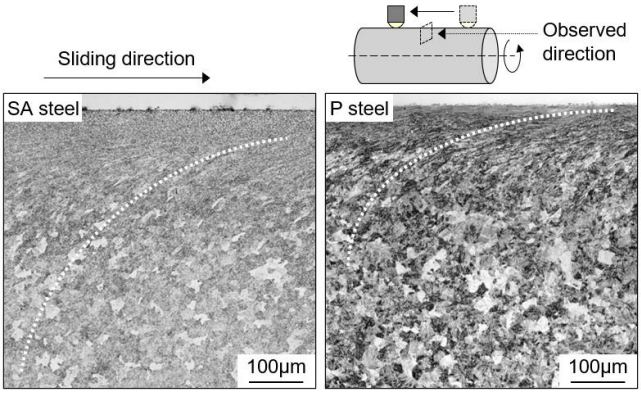

Figure 4 OM images of SA and P steels after 1-pass burnishing at the surface of round section.

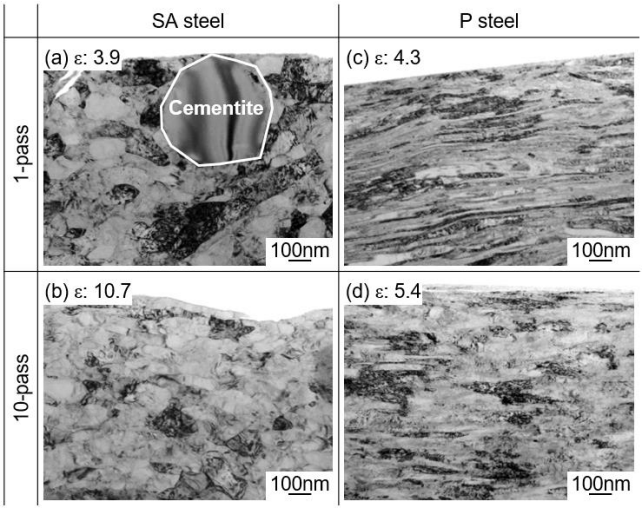

Figure 5 TEM images of SA and P steels after 1-pass and 10-pass burnishing at the surface of round section.

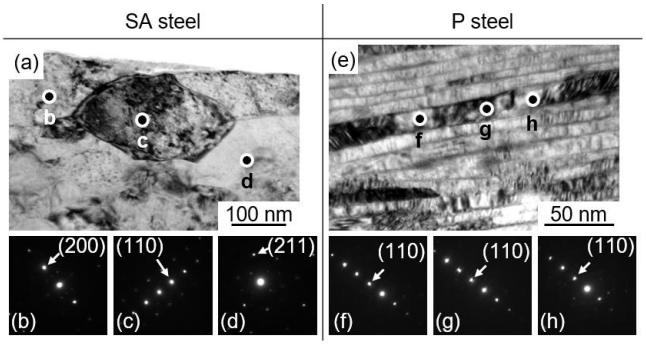

Figure 6 Diffraction analysis of adjacent ferrite grains of SA and P steels after 1-pass burnishing by TEM.

dynamic recrystallization process under burnishing. SA steel after 10-pass burnishing was also random oriented equiaxed grains, but the equivalent circle diameter was reduced to

130nm as shown Fig.5 (b).

In contrast, P steel maintained lamellar structure without equiaxed ultrafine ferrite grains even after 10-pass burnishing as shown Fig. 5 (c), (d). In addition, grain orientations of adjacent ferrite grains along the lamellar cementite were slightly rotated, and the grain boundaries were low angle boundaries as shown Fig. 6 (e)-(h). This indicates that continuous dynamic recrystallization of ferrite was suppressed in P steel.

Based on these results, the effect of carbide and ferrite morphology on the microstructural evolution by burnishing is discussed as follows. In SA steel, multiple dislocation slip system is activated by severe plastic deformation, and frequent cross slip forms dislocation cells and high angle grain boundaries. On the other hand, in P steel, active dislocation slip system is limited by lamellar structure even in severe plastic deformation. Therefore, cross slip and formation of dislocation cells are suppressed.

4. Conclusion

In this study, the ultrafine microstructural development under severe plastic deformation using burnishing in SA steel and P steel of AISI 52100 was investigated.

In SA steel, spherical cementite + ferrite microstructure, equiaxed ultrafine ferrite grains were formed at the burnished surface. These ultrafine grains were estimated to be formed by continuous dynamic recrystallization because of their high angle grain boundaries.

On the other hand, P steel, pearlite microstructure, maintained initial lamellar structure without equiaxed ultrafine ferrite grains even after 10-pass burnishing. Since the grain boundaries of adjacent ferrite grains along the lamellar cementite were low angle boundaries, active slip system was considered to be limited by the lamellar structure in P steel. Therefore, lamellar cementite was estimated to suppress the continuous dynamic recrystallization.

References

1) N. Tsuji, Y. Ito, Y. Saito, Y. Minamino: Scr. Mater. **47** (2002) 893-899.
2) N. Tsuji, S. Okuno, Y. Koizumi, Y. Minamino: Mater. Trans. **45** (2004) 2272-2281.
3) Y. Xu, Z. G. Liu, M. Umemoto and K. Tsuchiya: Metall. Mater. Trans. A, 39 (2002) 2195-2203.
4) J. Humphreys, G. S. Rohrer and A. Rolett: *Recrystallization and Related Aneeling Phenomena*, *3rd ed*., (Elsevier, Amsterdum, 2017) pp.471.
5) R. Gholizadeh, A. Shibata, N. Tsuji: Materialia **6** (2019) 100262.
6) M. Umemoto, Z. G. Liu, K. Masuyama, X. J. Hao and K. Tsuchiya: Scr. Mater. **44** (2001) 1741.
7) Y. Todaka, M. Umemoto, J. Yin, Z. Liu and K. Tsuchiya: Mater. Sci. Eng. A **462** (2007) 264.
8) Y. Todaka, M. Yoshii, M. Umemoto, C. Wang and K. Tsuchiya: Mater. Sci. Forum 584-586 (2008) 597.
9) Y. Todaka, M. Umemoto, S. Tanaka and K. Tsuchiya: Mater. Trans. **45** (2004) 2209-2213.